Cellular/Molecular

Abl2/Arg Controls Dendritic Spine and Dendrite Arbor Stability via Distinct Cytoskeletal Control Pathways

Yu-Chih Lin,[1] Mark F. Yeckel,[2,3] and Anthony J. Koleske[1,2,3]

Departments of [1]Molecular Biophysics and Biochemistry, and [2]Neurobiology, and [3]Interdepartmental Neuroscience Program, Yale University, New Haven, Connecticut 06520

Rho family GTPases coordinate cytoskeletal rearrangements in neurons, and mutations in their regulators are associated with mental retardation and other neurodevelopmental disorders (Billuart et al., 1998; Kutsche et al., 2000; Newey et al., 2005; Benarroch, 2007). Chromosomal microdeletions encompassing p190RhoGAP or its upstream regulator, the Abl2/Arg tyrosine kinase, have been observed in cases of mental retardation associated with developmental defects (Scarbrough et al., 1988; James et al., 1996; Takano et al., 1997; Chaabouni et al., 2006; Leal et al., 2009). Genetic knock-out of Arg in mice leads to synapse, dendritic spine, and dendrite arbor loss accompanied by behavioral deficits (Moresco et al., 2005; Sfakianos et al., 2007). To elucidate the cell-autonomous mechanisms by which Arg regulates neuronal stability, we knocked down Arg in mouse hippocampal neuronal cultures. We find that Arg knockdown significantly destabilizes dendrite arbors and reduces dendritic spine density by compromising dendritic spine stability. Inhibiting RhoA prevents dendrite arbor loss following Arg knockdown in neurons, but does not block spine loss. Interestingly, Arg-deficient neurons exhibit increased miniature EPSC amplitudes, and their remaining spines exhibit larger heads deficient in the actin stabilizing protein cortactin. Spine destabilization in Arg knockdown neurons is prevented by blocking NMDA receptor-dependent relocalization of cortactin from spines, or by forcing cortactin into spines via fusion to an actin-binding region of Arg. Thus, Arg employs distinct mechanisms to selectively regulate spine and dendrite stability: Arg dampens activity-dependent disruption of cortactin localization to stabilize spines and attenuates Rho activity to stabilize dendrite arbors.

Introduction

Dendritic spines are small protrusions that extend from dendrites in mature neurons (Tada and Sheng, 2006; Bourne and Harris, 2008). Because they serve as the main receptive contacts for excitatory neurons (Sorra and Harris, 2000), the long-term spine maintenance is essential for the structural stability of neuronal networks. Synaptic activity, neurotrophin signaling, and pairing of *trans*-synaptic adhesion receptors are all critical for long-term spine stability (Bourne and Harris, 2008; Yoshihara et al., 2009; Lin and Koleske, 2010; Benson and Huntley, 2012). In particular, activity-dependent morphogenesis and plasticity of spines provides the foundation for learning, memory, and adaptation of the brain (Zhang and Benson, 2000; Hering and Sheng, 2001; Nägerl et al., 2004; Saneyoshi et al., 2010). Signals generated by these events, such as calcium-dependent signaling, converge within the spine on cytoskeletal regulators, including the small Rho family GTPases (Smart and Halpain, 2000; Govek et al., 2005; Tada and Sheng, 2006; Hotulainen and Hoogenraad, 2010; Lin and Koleske, 2010; Svitkina et al., 2010; Tolias et al., 2011; Saneyoshi and Hayashi, 2012). Dysregulation of Rho GTPase regulators such as *OPHN1*, a RhoA inhibitor, or *ARHGEF6*, a Rac1 activator, disrupts spine morphogenesis and causes X-linked mental retardation (Billuart et al., 1998; Kutsche et al., 2000; Govek et al., 2004; Nodé-Langlois et al., 2006). Similarly, chromosomal microdeletions involving p190RhoGAP or its regulator, the Abl2/Arg tyrosine kinase, have been observed in cases of mental retardation associated with developmental defects (Scarbrough et al., 1988; James et al., 1996; Takano et al., 1997; Chaabouni et al., 2006; Leal et al., 2009).

Our previous studies highlighted the importance of Arg-mediated p190RhoGAP signaling in maintaining neuronal stability (Moresco et al., 2005; Sfakianos et al., 2007; Gourley et al., 2012; Warren et al., 2012). Synapses and dendrites develop normally on principal neurons in $arg^{-/-}$ mice, reaching their mature size by postnatal day 21 (P21) (Sfakianos et al., 2007; Gourley et al., 2012). However, $arg^{-/-}$ neurons exhibit significant synapse and spine loss by P31, followed by dendrite arbor regression and behavioral impairments by early adulthood. p190RhoGAP activity is reduced and Rho activity is elevated in $arg^{-/-}$ mice suggesting that elevated Rho activity causes synapse loss and dendrite regression. Intriguingly, reducing levels of Rho downstream effector ROCKII restores dendrite complexity but does not restore synapse or spine density in $arg^{-/-}$ mice (Sfakianos et al., 2007). This observation raised the fundamental question of how Arg controls spine stability.

Received Sept. 7, 2012; revised Nov. 30, 2012; accepted Dec. 1, 2012.

Author contributions: Y.-C.L., M.F.Y., and A.J.K. designed research; Y.-C.L. performed research; Y.-C.L., M.F.Y., and A.J.K. contributed unpublished reagents/analytic tools; Y.-C.L. analyzed data; Y.-C.L. and A.J.K. wrote the paper.

This project is supported by Public Health Service Grants NS39475 and CA133346 to A.J.K. We thank Drs. Pietro DeCamilli, Thomas Biederer, Sreeganga Chandra, Kevin Collins, Michael Higley, and Michael Koelle, as well as other members of the Koleske laboratory for their critical discussion and suggestions for this manuscript.

The authors declare no competing financial interests.

Correspondence should be addressed to Anthony J. Koleske, Department of Molecular Biophysics and Biochemistry, Interdepartmental Neuroscience Program, Yale University, New Haven, CT 06520. E-mail: anthony.koleske@yale.edu.

DOI:10.1523/JNEUROSCI.4284-12.2013

 0270-6474/13/331846-12$15.00/0

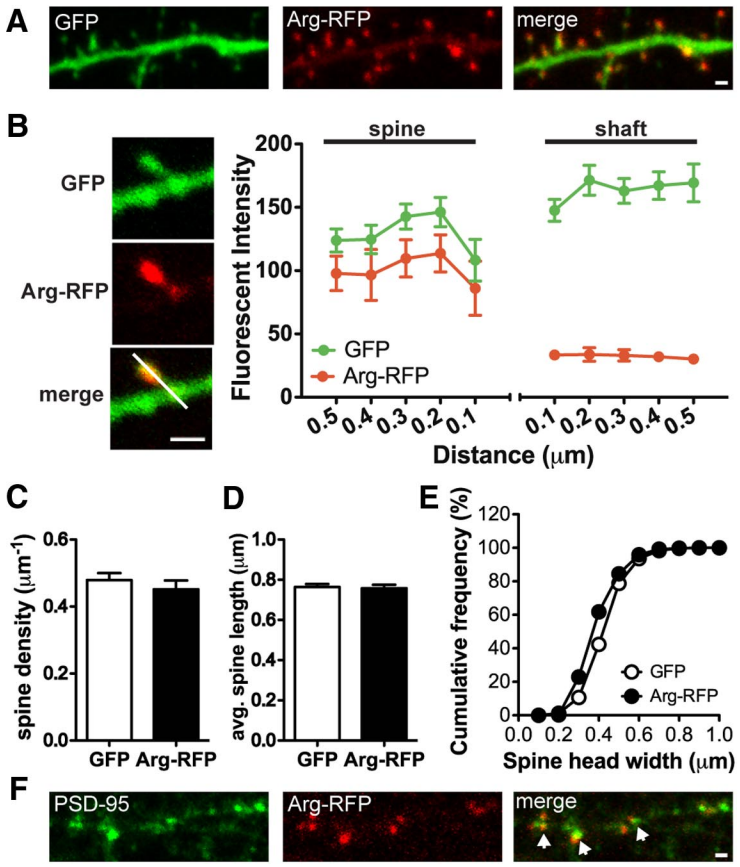

Figure 1. Arg is localized and enriched at dendritic spines. ***A***, Confocal images of a cultured hippocampal neuron at 18 DIV. The neuron was transfected with Arg-RFP and GFP. Scale bar, 1 μm. ***B***, Representative images of a dendritic spine. The quantification of Arg-RFP fluorescence intensity in the dendritic spine versus the dendrite shaft is shown. Fluorescence intensity of Arg-RFP and GFP across the spine and adjacent shaft was measured by a line scan (white line). Note that Arg-RFP is highly enriched in dendritic spines. ***C***, Spine density of GFP- or Arg-RFP-transfected neurons at 15 DIV. ***D***, ***E***, Averaged dendritic protrusion length (***D***) and cumulative frequency of spine head size (***E***), of GFP or Arg-RFP-transfected neurons. Note that Arg-RFP does not promote spine formation or changes in the spine length and width. ***F***, Confocal images of an Arg-RFP-transfected neuron immunostained with the postsynaptic marker PSD-95 (green). Note that Arg-RFP (red) is colocalized with PSD-95 puncta (arrows). Scale bar, 1 μm.

We demonstrate here that Arg confers spine stability by facilitating localization of the actin polymerization regulator and actin network stabilizer cortactin to spines. Inhibiting RhoA/ROCK signaling prevents dendrite arbor loss following Arg knockdown in neurons, but does not block spine loss. Time-lapse imaging reveals that Arg knockdown also destabilizes a subset of spines. The remaining spines exhibit larger heads and have increased synaptic strength. Cortactin levels are significantly reduced in the spines of Arg knockdown neurons, but blocking NMDA receptor (NMDAR) function prevents cortactin loss from spines in Arg knockdown neurons and restores spine stability. Most important, forcing cortactin to localize to spines via an Arg-cortactin fusion is sufficient to stabilize spines in Arg knockdown neurons. Together, these data indicate that Arg employs distinct cytoskeletal control mechanisms to selectively regulate dendritic spine and dendrite arbor stability.

Materials and Methods

Animals. BALB/c mice were purchased from Charles River Laboratories. Animals were housed and cared for in a Yale-sponsored Office for Protection from Research Risks approved animal facility. Neonatal mice of both sexes were killed for neuronal culture preparation. All procedures were approved by the Yale University Institutional Animal Care and Use Committee.

Plasmids. Arg-RFP, Arg-YFP, Abl-YFP, Arg557C-RFP, cortactin-RFP, and cortactinΔ SH3-Arg668C (cortactin-Arg fusion) were generated as previously reported (Miller et al., 2004; Lapetina et al., 2009; Peacock et al., 2010). RhoA19N plasmid was subcloned into the pZip vector. shRNAs targeted to mouse Abl2/Arg cDNA were generated and subcloned into the pLL3.7 vector (Rubinson et al., 2003). shArg3382 was generated by synthesizing two complementary oligonucleotides (5′-tgcctcag actcgcaacaagtttcaagagaacttgttgcgagtctgaggcttttttc-3′ and 5′-tcgagaaaaaagcctcagactcgcaacaagttctcttgaaacttgttgcgagtctgaggca-3′) and subcloned into the pLL3.7 vector between HpaI and XhoI sites. The shRNA-resistant Arg (Arg^r) construct was made by mutating three nucleotides in the shArg sequences with two PCR primers: 5′-ctcgtaataaatttgccttccgagaggctgtgagcaaactcgagcttagc-3′and5′-gctaagctcgagtttgctcacagcctctcggaaggcaaatttattacgag-3′. Arg^r was then subcloned into the N1-pEYFP vector or shArg plasmid, which allows shArg and Arg^r-GFP to be expressed in the same vector. These sequences were also mutated in the cortactin-Arg fusion to be resistant to Arg knockdown.

Cell culture and transfections. HEK-293 cells were plated in 6-well plates and maintained in high glucose DMEM (Invitrogen) growth media supplemented with 1% pen/strep (Invitrogen), 2 mM L-glutamine (Invitrogen), and 10% fetal bovine serum (Sigma-Aldrich). Primary neuronal cultures were prepared from P1 mouse hippocampus. Neurons were maintained in serum-free media containing 1% pen/strep, 2 mM L-glutamine, and 2% B27-supplement (Invitrogen) in neural basal media (Invitrogen). Glass coverslips in 24-well plates were coated with 20 μg/ml poly-(D)-lysine (BD Biosciences). Transfection was performed using a calcium-phosphate precipitation method in both HEK-293 cells and primary neurons. Y-27632 (100 μM; Sigma-Aldrich), 50 μM DL-2-amino-5-phosphono-valeric acid (APV) (Sigma-Aldrich), or 3 μM ifenprodil (Sigma-Aldrich) were added the day after transfection and incubated with neurons for 48 h before fixation.

Western blot analysis. Cells were harvested in lysis buffer containing 20 mM Tris, pH 7.5, 150 mM NaCl, 2 mM EDTA, 1% Triton X-100, and a phosphatase and protease inhibitor mixture. Protein concentration was determined using Pierce BCA Protein assay Kit (Thermo Scientific). Total protein (75 μg) from HEK-293 cell lysates was used to determine the knockdown efficiency. Protein samples were run on a 10% SDS-PAGE and transferred to a nitrocellulose membrane for immunoblotting with antibodies against GFP (Rockland) and β-actin (Abcam) in Tris-buffered saline—Tween 20 containing 3% milk. Densitometry of blotted protein was performed on scanned films using ImageJ (National Institutes of Health; NIH).

Immunocytochemistry and morphometric analysis. Neurons were fixed with 4% paraformaldehyde in PBS and permeabilized with 0.1% Triton X-100 and 3% bovine serum albumin in PBS. Cells were immunostained with primary antibodies against GFP (Rockland), RFP (Millipore Bioscience Research Reagents), cortactin (clone 4F11), and PSD-95 (NeuroMab), followed by Alexa 488- and 594-conjugated secondary antibodies (Invitrogen). F-actin was labeled with Alexa 647-conjugated phalloidin (Invitrogen) together with the incubation of secondary antibodies. For dendrite analysis, *z*-stack images were taken using an inverted fluorescent microscope (Nikon) with 40× NA 1.0 objective (Nikon; NIS Elements). For dendritic spine analysis, 2–3 dendrite segments per neuron were selected randomly from secondary or tertiary branches on the apical dendrite for imaging. Images were taken using a Zeiss LSM510 or

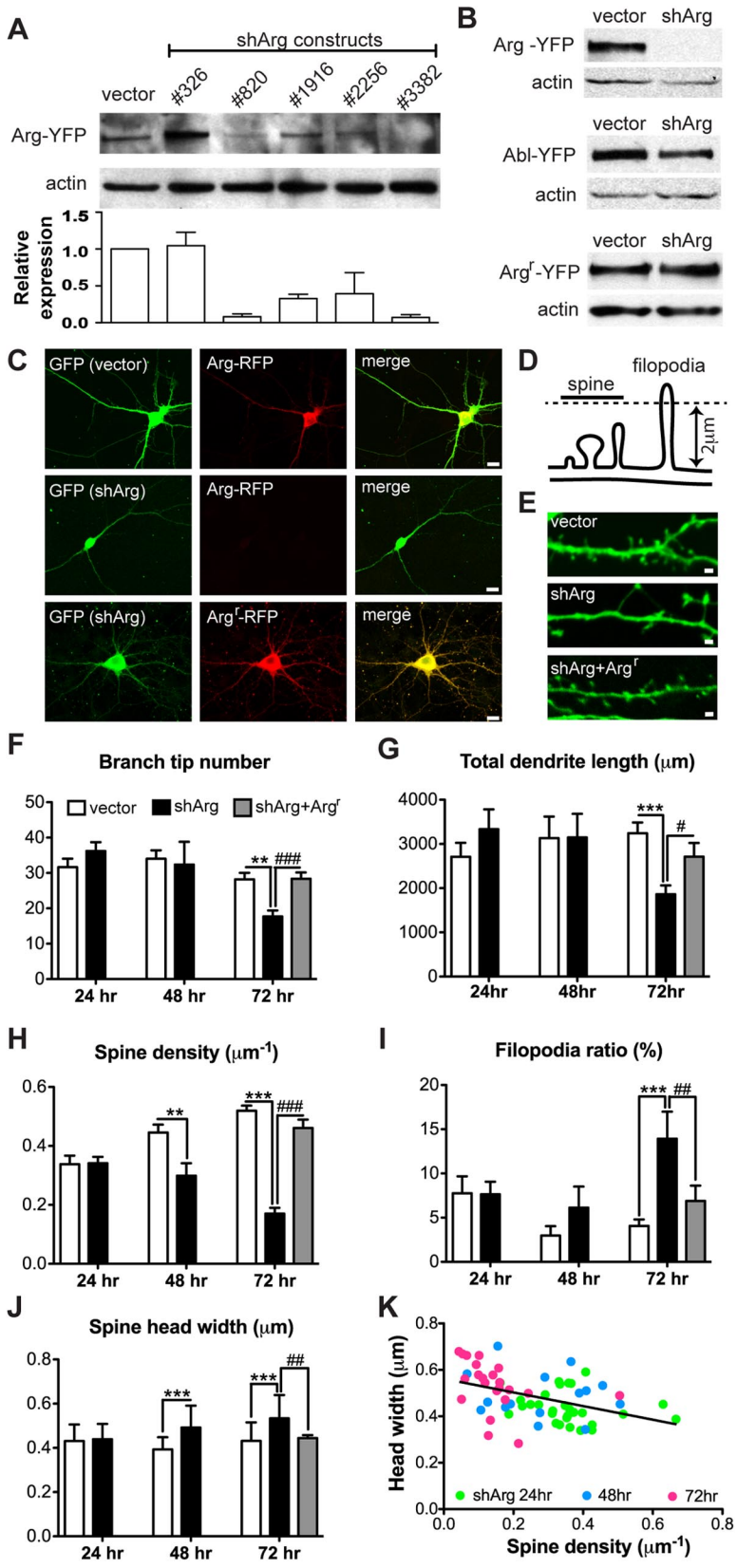

Figure 2. Arg knockdown collapses dendrite arbors and destabilizes dendritic spines. ***A***, Immunoblot analyses of Arg knockdown in HEK-293 cells. Cells were transfected with control vector or five different shRNA constructs together with Arg-YFP to determine Arg knockdown efficiency. shArg3382 (shArg) had the highest knockdown efficiency and was used for the following experiments. ***B***, HEK-293 cells were cotransfected with control vector or shArg together with Arg-YFP, Abl-YFP, or Arg^r-YFP for 72 h. shArg efficiently knocks down Arg-YFP, but not the related Abl-YFP or Arg^r-YFP. ***C***, Confocal images of cultured hippocampal neurons transfected with control vector or shArg. Neurons were cotransfected with Arg-RFP or Arg^r-RFP at 12 DIV and fixed 72 h after transfection. Neurons were immunostained with antibodies to GFP and RFP. shArg, but not the control vector, knocks down Arg-RFP in cultured neurons. Note that the dendrite arbors are smaller in neurons treated with shArg alone. Scale bar, 10 μm. ***D***, Illustration shows the criteria for distinguishing dendritic spines and filopodia. ***E***, Confocal images of dendritic spines from neurons transfected with control vector, shArg, or shArg with Arg^r. Scale bar, 1 μm. ***F–I***, Averaged dendrite branch tip number (***F***), total dendrite length (***G***), spine density (***H***), and filopodia ratio (***I***) of neurons transfected with vector or shArg analyzed at 24, 48, and 72 h after transfection. For shArg with Arg^r, only data analyzed at 72 h after transfection is shown. Arg knockdown neurons showed a reduction of dendrite branch tip numbers as well as total dendrite length at 72 h after transfection. These neurons also exhibit decreased spine density and an increase of filopodia ratio. Expression of shRNA-resistant Arg rescues these phenotypes in knockdown neurons. ***J***, Averaged spine head width of neurons transfected with control vector, shArg, and shArg with Arg^r. Arg knockdown neurons show enlargement of spine heads compared with control. $^{**}p < 0.01$, $^{***}p < 0.001$ when compared with control vector; $\#p < 0.05$, $\#\#p < 0.01$, $\#\#\#p < 0.001$ when compared with shArg. Two-way ANOVA with Bonferroni post-tests; $n = 20–37$ neurons, four independent cultures. ***K***, Correlation between spine density and spine head width in Arg knockdown neurons. Spine density correlates negatively with spine head width. $r = -0.4306$, $p = 0.0003$, $n = 66$ neurons.

LSM710 confocal microscope with 63× NA 1.4 objective and 4× zoom for spine analysis. Each morphological parameter was quantified using ImageJ (NIH) with LSM (http://rsbweb.nih.gov/ij/plugins/lsm-reader.html), NeuronJ (Meijering et al., 2004; Meijering, 2010), and Nikon ND2 Reader plug-ins (Nikon Instruments). Dendritic protrusion number, length, and width within a dendritic segment were measured and measurements from imaged segments were averaged for each neuron. Protrusion lengths >2 μm are defined as filopodia, while those are 2 μm or less are defined as spines (see Fig. 2*D*). All neurons measured within the same treatment group were averaged to obtain the averaged spine density, protrusion length, spine head width, and filopodia ratio (the percentage of filopodia in total protrusions counted) for that group. Spine head width was measured from all protrusions. Branch tip number and the total dendrite length were measured by tracing individual dendrites for each neuron. To measure the spine enrichment (spine index) of cortactin and F-actin content, a region of interest was selected in the dendritic spine and adjacent dendrite shaft. The fluorescence intensity of GFP, cortactin, F-actin, and cortactin-RFP was measured using Volocity software (PerkinElmer). Spine index = $[\text{RFP/GFP intensity}]_{\text{spine}}/[\text{RFP/GFP intensity}]_{\text{shaft}}$. Imaging and analysis were performed while blinded to experimental conditions. Data are reported as mean ± SEM and graphs were generated using GraphPad Prism 5. Statistical analyses were performed using appropriate test as indicated in figure legends. For Kolmogorov–Smirnov test, only $p < 0.001$ is considered as significantly different.

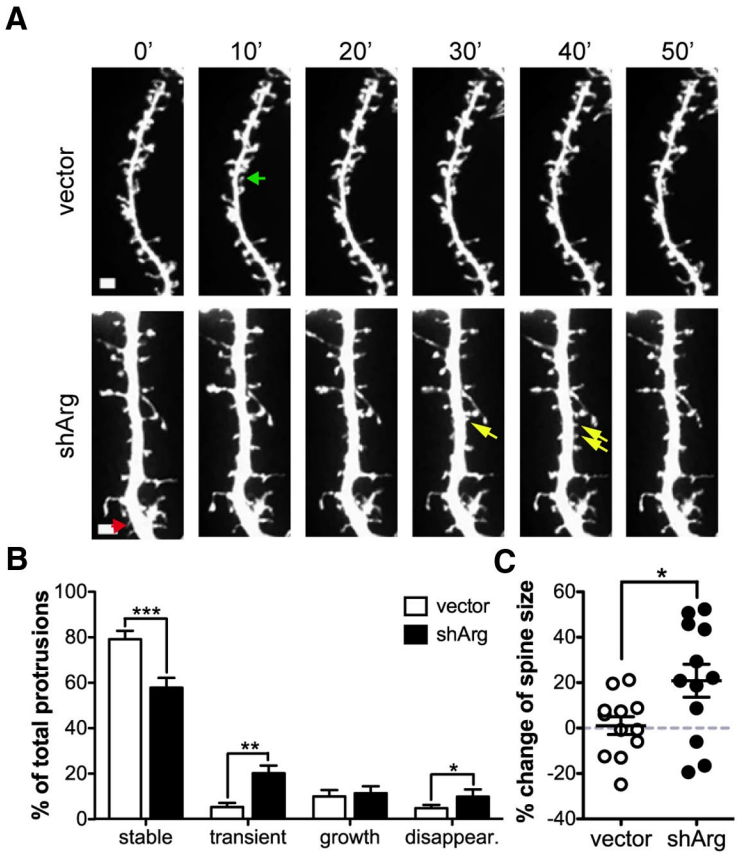

Figure 3. Arg knockdown neurons exhibit more dendritic spine destabilization events. ***A***, Confocal images of control vector or shArg-transfected neurons imaged with 10 min interval for 1 h. Examples of spine behavior are shown as colored arrows. Green, spine growth. The spine appears after the second frame and persists to the last frame. Red, Spine disappearance. The spine appears at the first frame but disappears at the last frame. Yellow, Transient spines. The spines are only evident in middle frames of the time-lapse series. Scale bar, 1 μm. ***B***, Quantification of the stable, transient, growth, and disappearance spines. ***C***, Within all stable spines, the averaged spine size change is shown. $^*p < 0.05$, $^{**}p < 0.01$, $^{***}p < 0.001$, unpaired Student's *t* test, $n = 12$ neurons.

Table 1. Total number counts and percentage breakdowns of protrusion types and behaviors

	Stable	Transient	Growth	Disappearance	Total
Vector	260 (78.4%)	18 (5.5%)	38 (10.1%)	14 (5.0%)	330
shArg	190 (58.0%)	55 (20.4%)	30 (11.6%)	31 (10.1%)	306

All protrusions that have appeared once during the 1 h imaging time were traced. Arg knockdown neurons exhibited less stable, but more transient and disappearance protrusions compared to control neurons. Note: The percentage is the averaged percentage from each group.

Live cell imaging. Control or shArg-transfected neurons were imaged at 36 h after transfection at room temperature. Cells were incubated in 8-well chambered slides (Thermo Scientific) with neural basal media without phenol red and supplemented with 20 μM HEPES during imaging. Time-lapse images were taken with 5 min intervals for 1 h using a Spinning Disk Confocal (Zeiss) with 100× NA 1.4 objective. Changes of spines were analyzed using ImageJ (NIH). Spines that were present at all times were defined as stable spines, spines not present at the first and the last frames but appearing in between were defined as transient spines, spines not present at the first frame but showed up at the last frame were defined as growth events, and spines present at the first frame but disappear at the last frame were defined as disappearance events. The percentage of spine size change at each time frame is normalized to the spine size at the first frame and averaged to a neuron.

Electrophysiology. Electrophysiological recordings of hippocampal neurons were performed at 48–72 h after transfection. Glass coverslips were transferred to a recording chamber continuously perfused with HEPES-buffered saline maintained at 32−34°C and containing the following (in mM): 150 NaCl, 3 KCl, 2 $CaCl_2{\cdot}2H_2O$, 10 HEPES, 5 dextrose, 1 μM tetrodotoxin, 10 μM glycine, and 0 mM Mg^{2+}; pH adjusted to 7.4 and osmolarity adjusted to match culture medium (~230–240 mOsm). Visualized whole-cell patch-clamp recordings were performed using infrared differential interference contrast microscopy on an upright microscope (Olympus BX51WI) with patch pipettes (3–5 MΩ) pulled from 2.0 mm outer diameter thick-walled borosilicate glass with filament. The pipettes were filled with the following (in mM): 134 $KMeSO_4$, 3 KCl, 10 HEPES, 1 $MgCl_2$, 4 Mg-ATP, 0.5 Na-GTP, 5 K_2-creatine phosphate, and 5 Na_2-creatine phosphate (pH 7.4, ~240 mOsm). Electrical signals were acquired at 20 kHz using an SEC 05LX amplifier (npi electronic) in discontinuous voltage-clamp mode (30–40 kHz switching frequency), digitized using custom written software (IGOR Pro; WaveMetrics), and analyzed off-line using AxoGraph X Scientific Software. The resting membrane potential of recorded neurons was between −40 and −50 mV; cells were held to −60 mV during recordings. Data were not corrected for liquid junction potential (~−11 mV). The threshold of the spontaneous miniature EPSCs (mEPSCs) was first determined manually based on the noise level (usually 2–5pA) (Kim and Tsien, 2008; Chen and Hsueh, 2012). Only events larger than 5 pA after thresholding were used for analyses (Helton et al., 2008). Only $p <$ 0.001 is considered as significantly different at Kolmogorov–Smirnov test.

Results

Arg is selectively enriched in dendritic spines

Abl2/Arg is a multidomain nonreceptor tyrosine kinase that is highly expressed in the CNS, where it is enriched at synapses (Koleske et al., 1998; Moresco and Koleske, 2003; Moresco et al., 2005). Despite repeated attempts, we could not detect endogenous Arg in neurons using immunofluorescence. Therefore, we exogenously expressed Arg-RFP to determine the cellular localization of Arg in cultured hippocampal neurons. Arg-RFP was selectively enriched in >90% of dendritic spines, while coexpressed GFP was found at comparable levels in both dendritic spines and dendrite shafts (Fig. 1*A*,*B*). We also found no significant differences in dendritic spine density, head width, or length in GFP-transfected control neurons versus Arg-RFP-transfected neurons (Fig. 1*C–E*). Thus, overexpressed Arg did not promote excess spine formation, nor markedly affect normal neuronal morphology. Although Arg-RFP localizes predominantly to the postsynaptic compartment, shown by its colocalization with the postsynaptic marker PSD-95 (Fig. 1*F*), residual levels of Arg have also been localized to presynaptic terminals (Moresco et al., 2003; Sfakianos et al., 2007), making it difficult to distinguish between the possible presynaptic versus postsynaptic contributions of Arg to neuronal stability.

Arg knockdown significantly compromises dendritic spine and dendrite arbor stability

To study how Arg cell-autonomously regulates spine and dendrite maintenance, we designed shRNAs to knock down Arg in cultured neurons. To first assess the efficiency and specificity of shArg, HEK-293 cells were transiently transfected with a

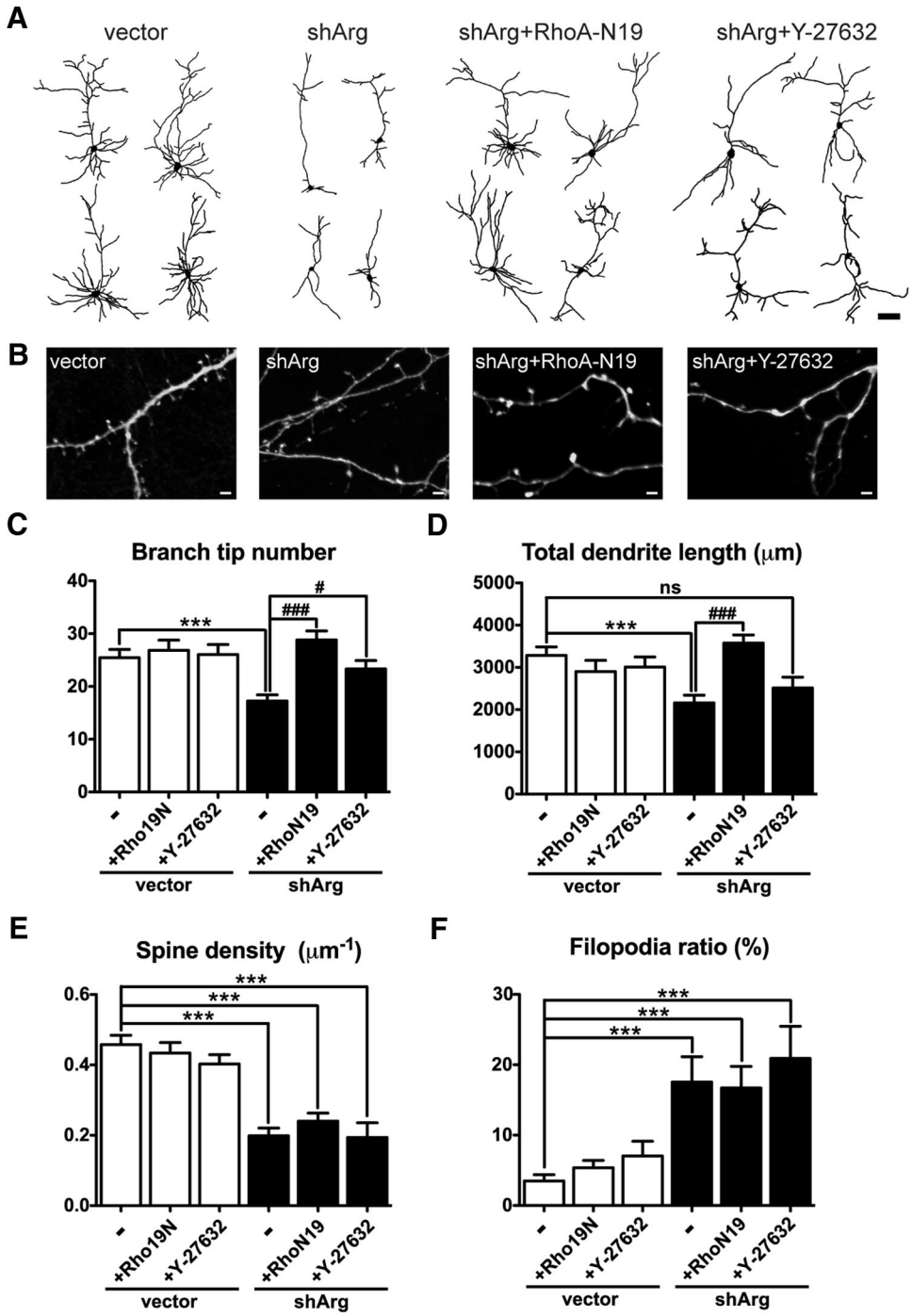

Figure 4. Rho inhibition protects against dendrite loss in Arg knockdown neurons. ***A***, Camera lucida drawings of dendrites from neurons transfected with vector, shArg, shArg with RhoA-N19, and transfected with shArg then treated with Y-27632. Scale bar, 100 μm. ***B***, Examples of Arg knockdown neurons with Rho blockade via RhoA-N19 expression or Y-27632 treatment. Arg knockdown neurons with inhibition of Rho signaling still have fewer dendritic spines compared with control neurons. Scale bar, 2 μm. ***C–F***, Dendrite branch tip number (***C***), total dendrite length (***D***), spine density (***E***), and filopodia ratio (***F***) in control- or shArg-transfected neurons. Coexpressing RhoA-N19 and Y-27632 treatment prevents dendrite arbor loss in Arg knockdown neurons. However, spine density and filopodia ratio are not affected. ***$p < 0.001$ when compared with control vector; #$p < 0.05$, ###$p < 0.001$ when compared with shArg, one-way ANOVA with post-Dunnett's multiple-comparison test. $n = 16–30$ neurons, three independent cultures.

functional Arg-yellow fluorescent protein (Arg-YFP) together with each shArg and knockdown efficiency was determined by immunoblot at 48–72 h after transfection. Two constructs targeting Arg base pairs 820–838 (shArg820) and 3382–3400 (shArg3382) yielded the highest knockdown efficiency (Fig. 2*A*). To further confirm the efficiency and specificity of shArg3382, we cotransfected it with Arg-YFP or the closely related Abl-YFP. This shArg efficiently knocked down Arg-YFP by >90%, but did not affect levels of Abl-YFP (Fig. 2*B*). Moreover, shArg3382 did not reduce levels of an engineered shRNA-resistant form of Arg, Arg^{r}-YFP (Fig. 2*B*). Knockdown efficiency was also confirmed in cultured neurons by coexpressing shArg3382 or a control vector with Arg-RFP. Arg-RFP fluorescence was reduced to undetectable levels upon

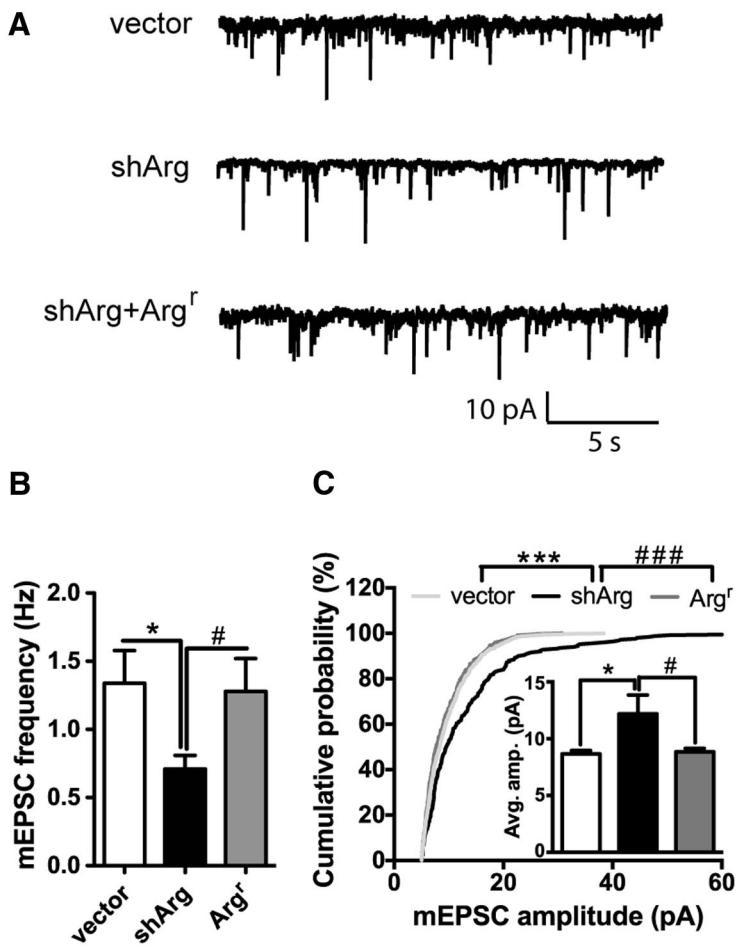

Figure 5. Synaptic transmission is elevated in Arg knockdown neurons. ***A***, Representative traces of mEPSCs recorded from neurons transfected with vector, shArg, or shArg with Arg^r. Scale bars: 10 pA and 5 s. ***B***, ***C***, Summary graphs show mEPSC frequency (***B***) and amplitude (***C***), respectively. Arg knockdown neurons show larger mEPSC amplitude and reduced frequency. *$p < 0.05$, ***$p < 0.001$ when compared with control vector; #$p < 0.05$; ###$p < 0.001$ when compared with shArg, unpaired Student's *t* test in ***B*** and ***C***, and Kolmogorov–Smirnov test in ***C***. $n = 9–14$ neurons, four independent cultures.

coexpression of shArg3382, while Arg^r-RFP expression was resistant to shArg3382 expression (Fig. 2*C*).

We transfected neurons with control vector or shArg at 12 d *in vitro* (DIV) and monitored spine and dendrite arbor stability at various time points by quantifying spine and dendrite arbor morphology in neurons. Both shArg820 and shArg3382 yielded similar neuronal phenotypes, but only data from shArg3382 (shArg from here on) are shown here. While control neurons maintained their dendrite arbors at 72 h after transfection (15 DIV), Arg knockdown neurons had 37% fewer branches (Fig. 2*F*) and a proportional decrease in total dendrite length (Fig. 2*G*). Unlike control neurons, which gradually increase in spine density within this period, Arg knockdown neurons lost spine density, with only 35% of control spine density remaining 72 h after transfection (Fig. 2*H*). A similar magnitude of destabilization was observed even 5 d after knockdown, and the neurons exhibited no signs of distress, indicating that the knockdown was not generally toxic to the neurons. As spines mature, they transform from a filopodium-like structure to a bulbous mushroom shape (Parnass et al., 2000; Yoshihara et al., 2009); therefore, filopodium-like spines typically represent a very small percentage of spines to the total population (Fig. 2*I*, filopodia ratio, see vector control). The reverse transition, i.e., from mushroom to filopodium-like, is believed to represent spine destabilization (Yoshihara et al., 2009; Lin and Koleske, 2010). In addition to reduced spine density, we found a twofold increase in the population of long filopodium-like protrusions in Arg knockdown neurons (Fig. 2*I*). While these neurons gradually lost dendritic spines, the head width of remaining spines became larger over time such that there was an inverse correlation between spine head size and spine density (Fig. 2*J*,*K*). In some cases these larger heads were attached to the shaft via a long filopodium-like neck (Fig. 2*E*). This inverse correlation of spine density with spine head size appears to be consistent with the observation that dendritic spines undergo a homeostatic change in size in response to stimulation or changes in spine density to maintain the balance of synaptic inputs (Konur et al., 2003; Bourne and Harris, 2011). Notably, all of these phenotypes in Arg knockdown neurons were prevented by coexpressing shRNA-resistant Arg (Arg^r) with shArg, which indicates that these phenotypes resulted from reduced Arg function.

We also performed time-lapse imaging at 36 h after transfection, midway through the period of spine loss following Arg knockdown to determine whether knockdown of Arg changes spine dynamics leading to destabilization of spines (Fig. 3*A*). Within a 1 h time frame, 80% of spines in control neurons were stable while only 58% of spines were stable in Arg knockdown neurons (Fig. 3*B*; Table 1). The percentage of transient spines, those appearing only within internal frames of the movies, increased to 20% in Arg knockdown neurons as compared with only 5% in control neurons. The percentage of spines that disappeared during the observation period was also increased twofold in Arg knockdown neurons relative to controls. In addition, the net size change of the stable spines in Arg knockdown neurons was significantly larger than control neurons and likely due to the increase of spine size ($p = 0.0257$; Fig. 3*C*). These data further indicate that spines in Arg knockdown neurons were less stable.

Inhibition of Rho signaling protects against dendrite loss in Arg knockdown neurons

arg$^{-/-}$ mice have reduced p190RhoGAP activity, leading to increased Rho signaling and premature synapse and dendrite loss. However, reducing gene dosage of the Rho effector ROCKII only rescued dendrite arbor complexity, but not synapse number in *arg*$^{-/-}$ mice (Sfakianos et al., 2007). To determine whether Rho signaling mediates the structural changes observed in Arg knockdown neurons, dominant-negative Rho (RhoA-N19) was coexpressed with shArg in cultured hippocampal neurons. RhoA-N19 protected against dendrite arbor loss in Arg knockdown neurons (Fig. 4*A*,*C*,*D*). However, expressing RhoA-N19 failed to block the reduction in spine density or the increase in filopodium-like spines in Arg knockdown neurons, leaving neurons with fully branched dendrite trees that were significantly impoverished in dendritic spines (Fig. 4*B*,*E*,*F*). Inhibition of the major Rho effec-

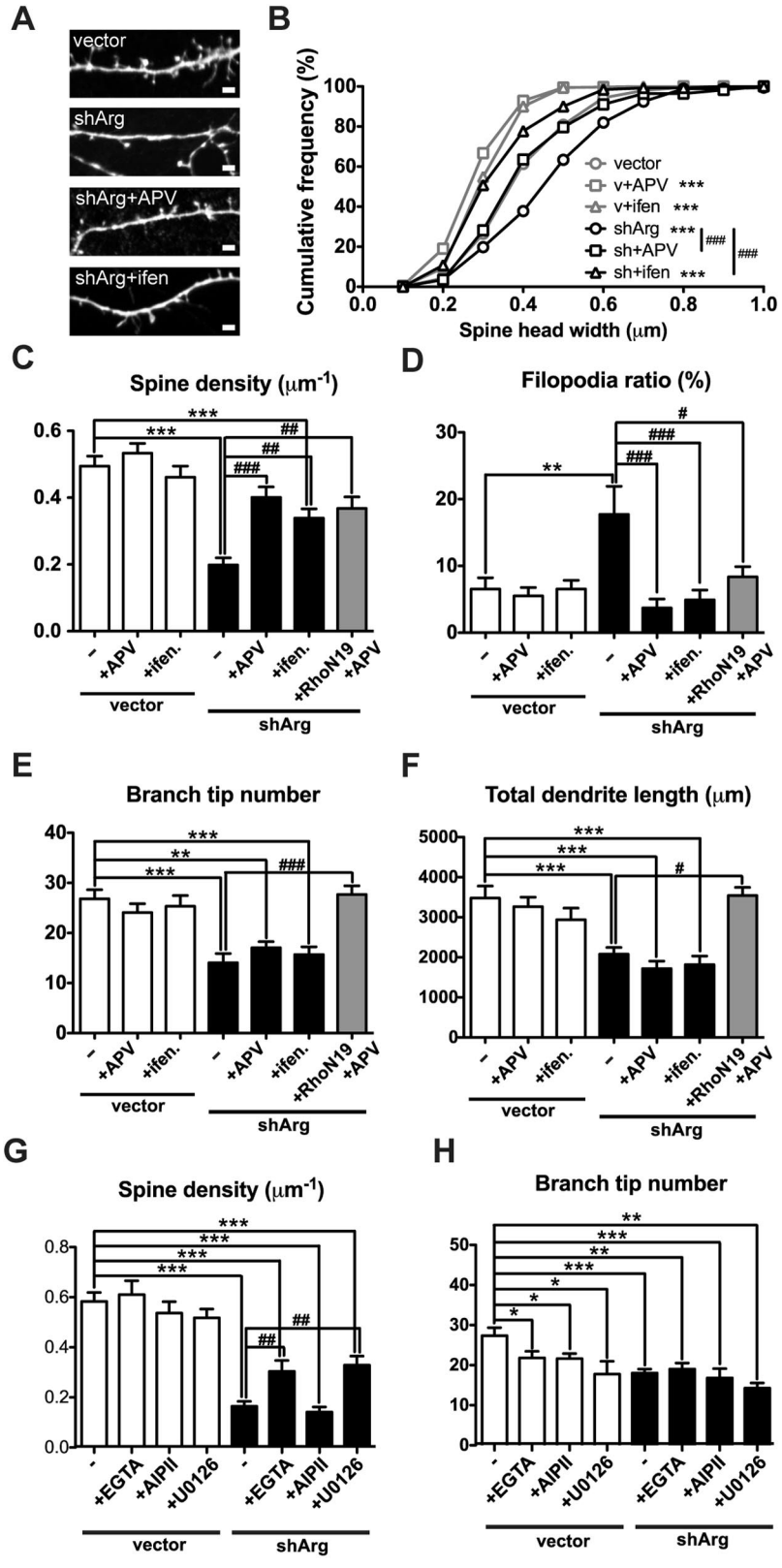

Figure 6. Blocking NMDAR function restores spine density. ***A***, Confocal images of neurons transfected with control or shArg vectors. Arg knockdown neurons were treated with 50 μM APV or 3 μM ifenprodil. ***B–F***, Spine head width (***B***), spine density (***C***), filopodia ratio (***D***), branch tip number (***E***), and total dendrite length (***F***) of vector- or shArg-transfected neurons treated with APV or ifenprodil. Treatment with APV or ifenprodil protects against spine loss and diminishes the increased filopodia ratio in Arg knockdown neurons. Arg neurons transfected with RhoA-N19 and treated with APV remain similar spine and dendrite stability as control neurons. $^{**}p < 0.01$, $^{***}p < 0.001$ when compared with control neurons without treatment; #<0.05, ##$p <$ 0.01, ###$p <$ 0.001 when compared with Arg knockdown neurons without treatment, one-way ANOVA with post-Dunnett's multiple-comparison test. $n = 16–31$ neurons, three independent cultures. ***G***, ***H***, Spine density (***G***) and dendrite branch tip number (***H***) of neurons transfected with vector control or shArg and treated with 10 μM EGTA, 1 μM AIP II, or 25 μM U0126. $^{*}p < 0.05$, $^{**}p < 0.01$, $^{***}p < 0.001$ when compared with untreated control; ##$p < 0.01$ when compared with Arg knockdown neurons, one-way ANOVA with post-Dunnett's multiple-comparison test. $n = 16–21$ neurons, three independent cultures.

tor Rho kinase (known as ROCKII in neurons) (Mueller et al., 2005; Kubo et al., 2008) using the ROCK inhibitor Y-27632 preserved dendrite branch tip numbers in Arg knockdown neurons (Fig. 4*A*,*C*), but did not completely restore dendrite arbor length (Fig. 4*D*), a pattern that mirrors the rescue of dendrite arbors by reducing ROCKII signaling in $arg^{-/-}$ mice (Sfakianos et al., 2007). Similar to the expression of RhoA-N19, ROCK inhibition did not prevent spine loss or the increased proportion of filopodia in Arg knockdown neurons (Fig. 4*B*,*E*,*F*). Consistent with previous reports (Nakayama et al., 2000; Suo et al., 2012; Xing et al., 2012), we found that expression of RhoA-N19 or treatment with Y-27632 had no significant effect on spine density or dendrite arbors in control neurons (Fig. 4*C–F*). Together, these results indicate that inhibiting Rho can supplant the function of Arg in stabilizing dendrite arbors but not its role in supporting spine stabilization. Thus, Arg must employ a distinct mechanism other than Rho signaling to control spine stability.

Arg knockdown neurons exhibit increased mEPSC amplitudes and NMDAR blockade restores spine stability

The findings that spine density is decreased and spine head width is increased in Arg knockdown neurons suggest they may exhibit changes in synaptic strength. To investigate whether changes in spine density and size were accompanied by changes in synapse strength, we measured mEPSCs of control and shArg-transfected neurons using whole-cell patch-clamp recording. Arg knockdown neurons had reduced mEPSC frequency compared with control neurons ($p = 0.0332$; Fig. 5*A*,*B*), consistent with the observed reduction in spine density. Strikingly, Arg knockdown neurons exhibited significantly larger mEPSC amplitudes compared with controls ($p = 0.0274$; Fig. 5*A*,*C*), consistent with their larger head size.

This increased synaptic strength in Arg knockdown neurons led us to hypothesize

←

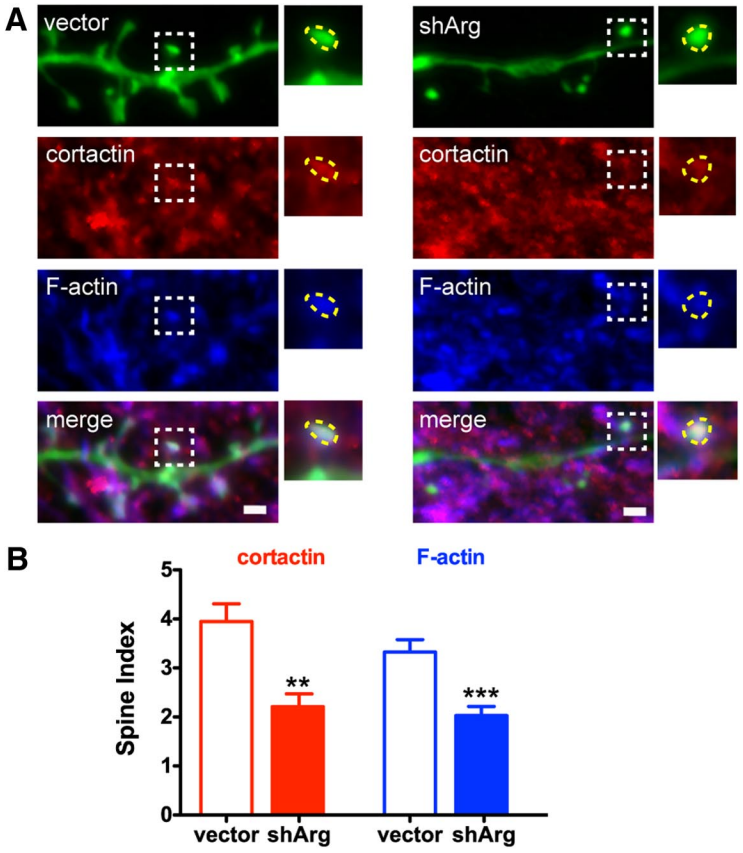

Figure 7. Cortactin localization and F-actin content is disrupted in Arg knockdown neurons. ***A***, Confocal images of neurons transfected with control vector or shArg. Neurons were immunostained with cortactin (red) and labeled with Alexa 647-phalloidin (blue). Higher magnification of a spine (white dashed box region) is shown as an example in the inset. Spine head is highlighted at yellow dashed region. Scale bar, 1 μm. ***B***, Spine index (relative fluorescence intensity in spines vs shafts) of cortactin and F-actin. $^{**}p < 0.01$, $^{***}p < 0.001$, unpaired Student's *t* test. $n = 19$ neurons, two independent cultures.

that excess activity, potentially mediated by NMDARs, may contribute to spine destabilization in these neurons. To test this hypothesis, Arg knockdown neurons were treated with the NMDAR antagonist APV. Blocking NMDAR function alters homeostasis in neurons and results in reduced spine head size, even in control neurons (Fig. 6*A*,*B*). However, consistent with the hypothesis, APV treatment prevented spine loss in Arg knockdown neurons, yielding spine density and percentage of filopodium-like protrusions that were indistinguishable from control neurons (Fig. 6*C*,*D*). Interestingly, APV treatment did not affect dendrite branch number or total dendrite arbor length (Fig. 6*E*,*F*). Blocking just GluN2B-containing NMDARs with ifenprodil was also sufficient to prevent spine destabilization in Arg knockdown neurons (Fig. 6*C*,*D*). Moreover, both dendrite and spine stability in Arg knockdown neurons were maintained when Rho signaling and NMDAR function were blocked simultaneously (Fig. 6*C*–*F*).

Increased synaptic strength is often accompanied by upregulation of intracellular calcium levels. We also tested whether blocking calcium influx following elevated synaptic activity was sufficient to prevent the spine destabilization. Depleting extracellular calcium with EGTA during the knockdown period partially stabilized spines in Arg knockdown neurons (Fig. 6*G*). Calcium influx in neurons activates both calcium/calmodulin-dependent protein kinase II (CaMKII) and mitogen-activated protein kinase (MAPK) pathways (Redmond, 2008). Inhibition of the MAPK pathway with U0126 partially restored spine stability in Arg knockdown neurons, while blocking CaMKII signaling with AIP II had no effect (Fig. 6*G*). Interestingly, blocking calcium signaling slightly but significantly reduced dendrite tip number (Fig. 6*H*), consistent with the role of calcium signaling in dendrite elaboration (Redmond, 2008). These data indicate that dysregulation of calcium influx and MAPK signaling also contributes to the spine destabilization observed in Arg knockdown neurons.

Cortactin localization is disrupted in Arg knockdown neurons, but is prevented by NMDAR antagonists

Our observation that blocking NMDAR activity and downstream signaling events rescues spine loss in Arg knockdown neurons raised the question of how elevated synaptic activity may lead to spine loss. The Arg binding partner cortactin (Boyle et al., 2007; Lapetina et al., 2009) has been shown to relocalize from spines to the dendrite shaft upon bath application of NMDAR agonists (Hering and Sheng, 2003; Iki et al., 2005; Chen and Hsueh, 2012). We reasoned that the increased NMDAR-mediated signaling in Arg knockdown neurons might trigger the exit of cortactin from spines, thereby inducing F-actin loss and spine destabilization. Consistent with this, both cortactin and F-actin content were reduced by 40% in spines from Arg knockdown neurons (Fig. 7*A*,*B*), suggesting that Arg facilitates cortactin localization to spines and that this interaction is crucial for stabilizing F-actin to maintain spine structure. Overexpression of a functional cortactin-RFP fusion protein was insufficient to rescue spine stability in Arg-deficient neurons (Fig. 8*D*), consistent with the reduced localization of cortactin-RFP in dendritic spines in these neurons relative to control neurons (Fig. 8*A*,*B*). Importantly, cortactin-RFP remained enriched in spines of Arg knockdown neurons treated with the NMDAR antagonist APV to the same extent as control neurons (Fig. 8*B*), consistent with their increased spine stability relative to untreated Arg knockdown neurons. Cortactin-RFP also restored spine head size to normal in Arg knockdown neurons (Fig. 8*E*), consistent with a previous report that cortactin overexpression causes smaller spine head size (Hering and Sheng, 2003).

Forced Arg–cortactin interactions prevent spine loss in Arg knockdown neurons

The finding that NMDA blockers prevented cortactin relocalization and spine loss in Arg knockdown neurons suggests that Arg-mediated control of cortactin localization to spines may be key to maintaining their stability. To test this hypothesis, we forced Arg-cortactin interactions using a fusion of cortactin lacking its SH3 domain to the Arg C-terminal actin-binding domains (cortactin-ΔSH3-Arg668-C) to create an "Arg-activated" cortactin (cort-Arg; Fig. 8*C*). This cort-Arg fusion protein localizes to actin-based protrusions in non-neuronal cells and partly rescues defective cell edge protrusion of both Arg knock-out and cortactin knockdown fibroblasts (Lapetina et al., 2009). The cort-Arg fusion protein

apparently mimics an Arg-bound cortactin conformation to allow more cortactin to bind to F-actin and promote formation or stability of F-actin networks (MacGrath and Koleske, 2012a). Importantly, this cortactin-Arg fusion protein is highly enriched in spines (Fig. 8*A*,*B*) and it prevents the spine loss and corrected spine head size in Arg knockdown neurons (Fig. 8*D*,*E*). Expressing the Arg C terminus alone (Arg557C) or the full-length cortactin did not prevent spine loss in Arg knockdown neurons. Together, these data support a model in which Arg stabilizes spines by promoting cortactin recruitment and function within spines, most likely by recruiting it to F-actin.

Discussion

Although dendritic spine formation and dendrite arbor development are intimately linked in developing neurons, spine and dendrite arbor stability become uncoupled in the mature nervous system. This uncoupling provides the neuron with gross morphological stability, while allowing for synaptic plasticity at individual dendritic spines (Holtmaat and Svoboda, 2009). Nevertheless, very little is known about the mechanisms that allow for the independent control of dendritic spine versus dendrite arbor stability. Our results demonstrate that Arg is critical for dendrite maintenance by attenuating RhoA activity to stabilize dendrite arbors. At the same time, Arg maintains the stability of dendritic spines by regulating localization of the important actin regulator, cortactin, to the spine. Thus, Arg is a key regulator of neuronal structural stability that acts via distinct mechanisms to mediate dendritic spine and dendrite arbor stabilization. These functions of Arg likely allow for short-term spine plasticity via changes in neurotransmission and actin remodeling, while preserving long-term dendrite arbor stability within mature neuronal circuits.

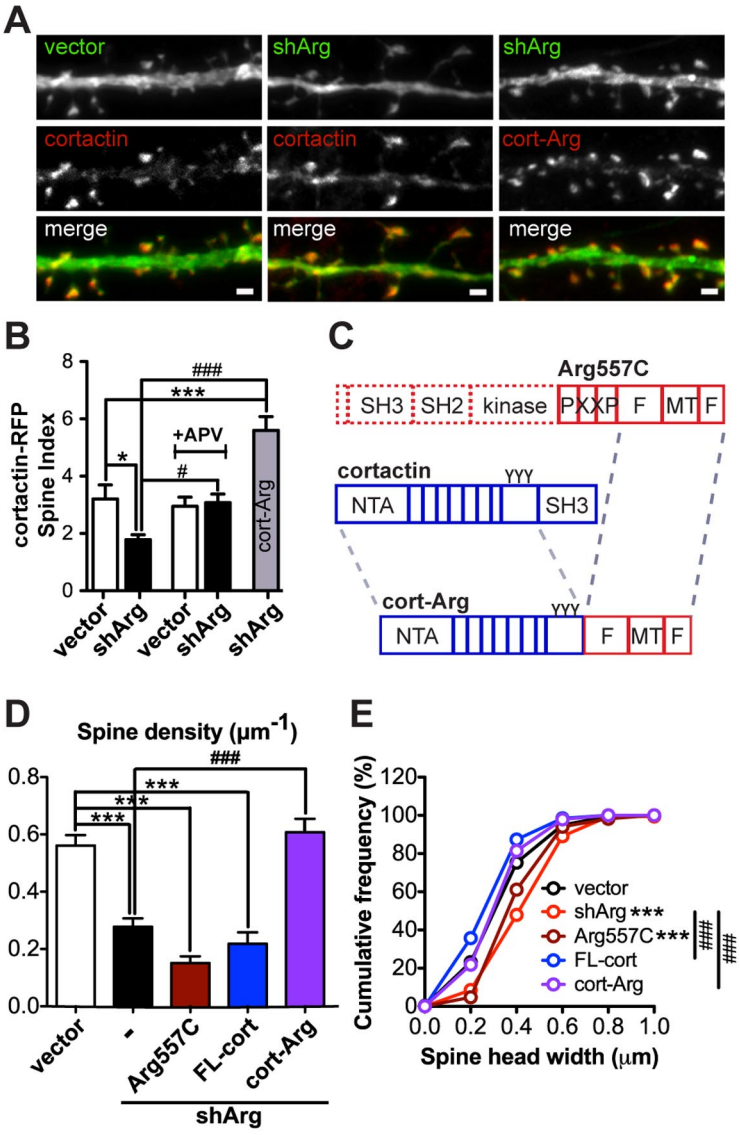

Figure 8. Forcing cortactin-Arg interactions prevents spine loss. ***A***, Examples of cortactin-RFP (red) or cortactin-Arg-RFP fusion protein (red) localization in control or Arg knockdown neurons. Scale bar, 1 μm. ***B***, Spine enrichment of cortactin-RFP or cortactin-Arg-RFP in neurons. Neurons treated with or without 50 μM APV. $n = 16–21$ neurons, three independent cultures. $^{*}p < 0.05$, $^{***}p < 0.001$ when compared with control vector; $\#p < 0.05$, $\#\#\#p < 0.001$ when compared with shArg, one-way ANOVA with post-Dunnett's multiple-comparison test. ***C***, Schematic structure of Arg557C, full-length cortactin, and cortactin-Arg (cort-Arg) fusion protein. The cort-Arg fusion protein is constructed by fusing cortactin lacking its SH3 domain with Arg lacking the N-terminal and PXXP motif (Arg-668C). ***D***, Spine density of vector- or shArg-transfected neurons. Arg knockdown neurons were complemented with the Arg557C domain (dark red), full-length cortactin (FL-cort; blue), and cort-Arg fusion (purple). Cort-Arg restores spine density in Arg knockdown neurons. $^{***}p < 0.001$ when compared with control neurons; $\#\#\#p < 0.001$ when compared with Arg knockdown neurons, one-way ANOVA with post-Dunnett's multiple-comparison test. $n = 28–42$ neurons, four independent cultures. ***E***, Cumulative frequency of spine head width of vector- or shArg-transfected neurons complemented with constructs as indicated in ***D***. $^{***}p < 0.001$ when compared with control; $\#\#\#p < 0.001$ when compared with shArg, Kolmogorov–Smirnov test.

Arg-mediated Rho inhibition selectively controls dendrite stability

Rho signaling has been implicated in the regulation of both spine and dendrite stability, but the reported contributions of RhoA or ROCK to these processes have varied greatly in different studies. Depending on the developmental time point examined or the structural definition of spines, some have reported an increase in spine density following inhibition of RhoA/ROCK signaling in neurons(Tashiro et al., 2000; Zhang and Macara, 2008; Kang et al., 2009) while some find spine density unchanged or reduced (Nakayama et al., 2000; Tashiro and Yuste, 2004; Schubert et al., 2006; Suo et al., 2012; Xing et al., 2012). Reducing gene dose of ROCKII in $arg^{-/-}$ mice restored dendrite complexity, but did not restore synapse density (Sfakianos et al., 2007). Here, for the first time, we knocked down Arg in cultured neurons and our data further suggest that Arg-mediated Rho inhibition has minimal effects on spine stability, while it selectively regulates the stability of dendrite arbors. Although p190RhoGAP has been localized to spines (Lamprecht et al., 2002; Sfakianos et al., 2007), p190RhoGAP is also detected in other regions of neurons (Lamprecht et al., 2002; Zhang and Macara, 2008). In fact, p190RhoGAP has also been shown to be downstream target of Par6, a polarity protein, and dominant-negative RhoA is sufficient to restore spine density in Par6 knockdown neurons (Zhang and

Macara, 2008). These observations raise the possibility that Arg and Par6 may exert differential spatial regulation of p190RhoGAP within the neuron. Moreover, our data suggest that Arg acts via a mechanism distinct from Rho inhibition to control spine stability.

Arg facilitates cortactin localization to the spine to confer spine stability

Dendritic spines are F-actin-rich structures and thus, the actin cytoskeleton dictates spine shape, size, and stability (Fischer et al., 1998, 2000; Matus, 2000; Schubert et al., 2006; Alvarez and Sabatini, 2007; Hotulainen and Hoogenraad, 2010). Cortactin is a key regulator of actin polymerization and actin stability (Daly, 2004; MacGrath and Koleske, 2012b). In neurons, cortactin is enriched in dendritic spines and this spine-targeting feature depends on its F-actin binding domain (Hering and Sheng, 2003). Arg binds to cortactin via at least two sets of reciprocal protein: protein interactions—the cortactin SH3 domain binds to a Pro-X-X-Pro-X-X-Pro motif in Arg, while the Arg SH2 domain can bind to tyrosine-phosphorylated cortactin (Lapetina et al., 2009; Liu et al., 2012). In addition to these direct interactions, Arg binding to F-actin stabilizes actin filaments and the Arg C-terminal F-actin binding domain promotes cortactin binding to F-actin (MacGrath and Koleske, 2012a), most likely by locally changing actin filament conformation (Galkin et al., 2005). Thus, losing Arg may directly destabilize actin filaments within the spine and also reduce cortactin binding to F-actin, resulting in destabilization of spine actin and loss of dendritic spines. However, a recent study shows that high concentration of cortactin inhibits actin branching (Siton et al., 2011). Therefore, overexpressing cortactin may minimize the spine head size in general (Hering and Sheng, 2003) and consequently "correct" spine head size in Arg knockdown neurons.

Several studies have also shown that robust glutamatergic stimulation drives cortactin out of the spine, resulting in spine dissolution (Hering and Sheng, 2003; Iki et al., 2005; Chen and Hsueh, 2012). We show here that Arg deficiency also increases synaptic activity and this may further exacerbate the localization and function of cortactin local in spines. Indeed, we find that blocking NMDAR activity with APV is sufficient to relocalize cortactin to spines and restore spine density to Arg knockdown neurons. Moreover, forcing Arg:cortactin interactions via direct fusion of portions of both molecules has an even stronger effect than APV treatment on spine localization and spine stability. These data strongly reinforce a model in which Arg-mediated stabilization of cortactin localization to actin in spines is key to maintaining spine stability.

How does Arg selectively mediate dendritic spine versus dendrite arbor stabilization?

Our finding that Arg can inhibit Rho signaling to stabilize dendrite arbors and facilitate cortactin localization in spines to stabilize spines raises the question of how one protein selectively regulates two distinct pathways to mediate neuronal stability. In addition to its kinase domain, Arg is a multifunctional adapter protein containing both F-actin- and microtubule-binding and protein-interaction motifs (Bradley and Koleske, 2009). Arg likely uses these domains to differentially interface with key effectors to execute different functions. For example, the Arg N-terminal half alone, which contains its kinase domain, is sufficient to mediate phosphorylation of p190RhoGAP and inhibition of Rho (Hernández et al., 2004; Bradley et al., 2006). This module mediates dendrite arbor stabilization (Sfakianos et al., 2007; Warren et al., 2012). In addition, Arg also uses domains in its unique C-terminal half to interact with cytoskeletal proteins, including cortactin, that are known to be required for spine plasticity and stability (Hering and Sheng, 2003; Ryu et al., 2006; Boyle and Koleske, 2007; Lapetina et al., 2009; Chen and Hsueh, 2012). Interactions between Arg and distinct substrates and binding partners may also be influenced by differential engagement with upstream regulators including integrins (Moresco et al., 2005; Warren et al., 2012), and possibly glutamate receptors, which may control Arg localization or activation within discrete signaling niches.

Disruption of neuronal stabilization by Arg signaling pathways may contribute to mental retardation

RhoA has been shown to play an antagonistic role in spine and dendrite stability such that RhoA/ROCK inhibition results in spine elongation and an increased dendrite arborization (Nakayama et al., 2000; Tashiro et al., 2000; Govek et al., 2004; Tashiro and Yuste, 2004; Van Aelst and Cline, 2004; Schubert et al., 2006; Iida et al., 2007; Zhang and Macara, 2008; Kang et al., 2009; Gisselsson et al., 2010). Nonetheless, disruption of Rho signaling pathway components, including Rho GTPase regulators, has been linked to mental retardation in humans, which is associated with defects in spine and dendrite morphology (Newey et al., 2005; Benarroch, 2007). $arg^{-/-}$ mice have elevated Rho activity and synapse and dendritic spine loss and dendrite atrophy, accompanied by significant deficits in behavior, learning, and memory (Sfakianos et al., 2007; Gourley et al., 2009, 2012). Similarly, reducing or eliminating Arg function in humans may disrupt neuronal structure and cause neurodevelopmental defects. In fact, chromosomal microdeletions that include the coding regions of Arg and p190RhoGAP have been observed in cases of mental retardation associated with developmental defects (Scarbrough et al., 1988; James et al., 1996; Takano et al., 1997; Chaabouni et al., 2006; Leal et al., 2009). It is presently unclear whether mutations or polymorphisms in genes encoding Arg signaling pathway components (e.g., integrin β1, Arg, or p190RhoGAP) also contribute to neurodevelopmental disorders in humans.

Summary

These studies demonstrate, for the first time, that Arg acts cell autonomously and employs distinct mechanisms to control dendrite arbor versus dendritic spine stability. Our results indicate that Arg dampens activity-dependent disruption of cortactin localization to stabilize spines, and attenuates Rho activity to stabilize dendrite arbors. Future studies will reveal the extent to which disruption or dysregulation of these mechanisms contributes to neurodevelopmental and neurodegenerative diseases in humans.

References

Alvarez VA, Sabatini BL (2007) Anatomical and physiological plasticity of dendritic spines. Annu Rev Neurosci 30:79–97. CrossRef Medline

Benarroch EE (2007) Rho GTPases: role in dendrite and axonal growth, mental retardation, and axonal regeneration. Neurology 68:1315–1318. CrossRef Medline

Benson DL, Huntley GW (2012) Building and remodeling synapses. Hippocampus 22:954–968. CrossRef Medline

Billuart P, Bienvenu T, Ronce N, des Portes V, Vinet MC, Zemni R, Roest Crollius H, Carri é A, Fauchereau F, Cherry M, Briault S, Hamel B, Fryns JP, Beldjord C, Kahn A, Moraine C, Chelly J (1998) Oligophrenin-1 encodes a rhoGAP protein involved in X-linked mental retardation. Nature 392:923–926. CrossRef Medline

Bourne JN, Harris KM (2008) Balancing structure and function at hippocampal dendritic spines. Annu Rev Neurosci 31:47–67. CrossRef Medline

Bourne JN, Harris KM (2011) Coordination of size and number of excitatory and inhibitory synapses results in a balanced structural plasticity along mature hippocampal CA1 dendrites during LTP. Hippocampus 21:354–373. CrossRef Medline

Boyle SN, Koleske AJ (2007) Use of a chemical genetic technique to identify myosin IIb as a substrate of the Abl-related gene (Arg) tyrosine kinase. Biochemistry 46:11614–11620. CrossRef Medline

Boyle SN, Michaud GA, Schweitzer B, Predki PF, Koleske AJ (2007) A critical role for cortactin phosphorylation by Abl-family kinases in PDGF-induced dorsal-wave formation. Curr Biol 17:445–451. CrossRef Medline

Bradley WD, Koleske AJ (2009) Regulation of cell migration and morphogenesis by Abl-family kinases: emerging mechanisms and physiological contexts. J Cell Sci 122:3441–3454. CrossRef Medline

Bradley WD, Hernández SE, Settleman J, Koleske AJ (2006) Integrin signaling through Arg activates p190RhoGAP by promoting its binding to p120RasGAP and recruitment to the membrane. Mol Biol Cell 17:4827–4836. CrossRef Medline

Chaabouni M, Martinovic J, Sanlaville D, Attié-Bittach T, Caillat S, Turleau C, Vekemans M, Morichon N (2006) Prenatal diagnosis and molecular characterization of an interstitial 1q24.2q25.2 deletion. Eur J Med Genet 49:487–493. CrossRef Medline

Chen YK, Hsueh YP (2012) Cortactin-binding protein 2 modulates the mobility of cortactin and regulates dendritic spine formation and maintenance. J Neurosci 32:1043–1055. CrossRef Medline

Daly RJ (2004) Cortactin signalling and dynamic actin networks. Biochem J 382:13–25. CrossRef Medline

Fischer M, Kaech S, Knutti D, Matus A (1998) Rapid actin-based plasticity in dendritic spines. Neuron 20:847–854. CrossRef Medline

Fischer M, Kaech S, Wagner U, Brinkhaus H, Matus A (2000) Glutamate receptors regulate actin-based plasticity in dendritic spines. Nat Neurosci 3:887–894. CrossRef Medline

Galkin VE, Orlova A, Koleske AJ, Egelman EH (2005) The Arg non-receptor tyrosine kinase modifies F-actin structure. J Mol Biol 346:565–575. CrossRef Medline

Gisselsson L, Toresson H, Ruscher K, Wieloch T (2010) Rho kinase inhibition protects CA1 cells in organotypic hippocampal slices during in vitro ischemia. Brain Res 1316:92–100. Medline

Gourley SL, Koleske AJ, Taylor JR (2009) Loss of dendrite stabilization by the Abl-related gene (Arg) kinase regulates behavioral flexibility and sensitivity to cocaine. Proc Natl Acad Sci U S A 106:16859–16864. CrossRef Medline

Gourley SL, Olevska A, Warren MS, Taylor JR, Koleske AJ (2012) Arg kinase regulates prefrontal dendritic spine refinement and cocaine-induced plasticity. J Neurosci 32:2314–2323. CrossRef Medline

Govek EE, Newey SE, Akerman CJ, Cross JR, Van der Veken L, Van Aelst L (2004) The X-linked mental retardation protein oligophrenin-1 is required for dendritic spine morphogenesis. Nat Neurosci 7:364–372. CrossRef Medline

Govek EE, Newey SE, Van Aelst L (2005) The role of the Rho GTPases in neuronal development. Genes Dev 19:1–49. CrossRef Medline

Helton TD, Otsuka T, Lee MC, Mu Y, Ehlers MD (2008) Pruning and loss of excitatory synapses by the parkin ubiquitin ligase. Proc Natl Acad Sci U S A 105:19492–19497. CrossRef Medline

Hering H, Sheng M (2001) Dendritic spines: structure, dynamics and regulation. Nat Rev Neurosci 2:880–888. CrossRef Medline

Hering H, Sheng M (2003) Activity-dependent redistribution and essential role of cortactin in dendritic spine morphogenesis. J Neurosci 23:11759–11769. Medline

Hernández SE, Settleman J, Koleske AJ (2004) Adhesion-dependent regulation of p190RhoGAP in the developing brain by the Abl-related gene tyrosine kinase. Curr Biol 14:691–696. CrossRef Medline

Holtmaat A, Svoboda K (2009) Experience-dependent structural synaptic plasticity in the mammalian brain. Nat Rev Neurosci 10:647–658. CrossRef Medline

Hotulainen P, Hoogenraad CC (2010) Actin in dendritic spines: connecting dynamics to function. J Cell Biol 189:619–629. CrossRef Medline

Iida J, Ishizaki H, Okamoto-Tanaka M, Kawata A, Sumita K, Ohgake S, Sato Y, Yorifuji H, Nukina N, Ohashi K, Mizuno K, Tsutsumi T, Mizoguchi A, Miyoshi J, Takai Y, Hata Y (2007) Synaptic scaffolding molecule alpha is a scaffold to mediate N-methyl-D-aspartate receptor-dependent RhoA activation in dendrites. Mol Cell Biol 27:4388–4405. CrossRef Medline

Iki J, Inoue A, Bito H, Okabe S (2005) Bi-directional regulation of postsynaptic cortactin distribution by BDNF and NMDA receptor activity. Eur J Neurosci 22:2985–2994. CrossRef Medline

James C, Jauch A, Robson L, Watson N, Smith A (1996) A 3 1/2 year old girl with distal trisomy 19q defined by FISH. J Med Genet 33:795–797. CrossRef Medline

Kang MG, Guo Y, Huganir RL (2009) AMPA receptor and GEF-H1/Lfc complex regulates dendritic spine development through RhoA signaling cascade. Proc Natl Acad Sci U S A 106:3549–3554. CrossRef Medline

Kim J, Tsien RW (2008) Synapse-specific adaptations to inactivity in hippocampal circuits achieve homeostatic gain control while dampening network reverberation. Neuron 58:925–937. CrossRef Medline

Koleske AJ, Gifford AM, Scott ML, Nee M, Bronson RT, Miczek KA, Baltimore D (1998) Essential roles for the Abl and Arg tyrosine kinases in neurulation. Neuron 21:1259–1272. CrossRef Medline

Konur S, Rabinowitz D, Fenstermaker VL, Yuste R (2003) Systematic regulation of spine sizes and densities in pyramidal neurons. J Neurobiol 56:95–112. CrossRef Medline

Kubo T, Yamaguchi A, Iwata N, Yamashita T (2008) The therapeutic effects of Rho-ROCK inhibitors on CNS disorders. Ther Clin Risk Manag 4:605–615. Medline

Kutsche K, Yntema H, Brandt A, Jantke I, Nothwang HG, Orth U, Boavida MG, David D, Chelly J, Fryns JP, Moraine C, Ropers HH, Hamel BC, van Bokhoven H, Gal A (2000) Mutations in ARHGEF6, encoding a guanine nucleotide exchange factor for Rho GTPases, in patients with X-linked mental retardation. Nat Genet 26:247–250. CrossRef Medline

Lamprecht R, Farb CR, LeDoux JE (2002) Fear memory formation involves p190 RhoGAP and ROCK proteins through a GRB2-mediated complex. Neuron 36:727–738. CrossRef Medline

Lapetina S, Mader CC, Machida K, Mayer BJ, Koleske AJ (2009) Arg interacts with cortactin to promote adhesion-dependent cell edge protrusion. J Cell Biol 185:503–519. CrossRef Medline

Leal T, Andrieux J, Duban-Bedu B, Bouquillon S, Brevière GM, Delobel B (2009) Array-CGH detection of a de novo 0.8Mb deletion in 19q13.32 associated with mental retardation, cardiac malformation, cleft lip and palate, hearing loss and multiple dysmorphic features. Eur J Med Genet 52:62–66. CrossRef Medline

Lin YC, Koleske AJ (2010) Mechanisms of synapse and dendrite maintenance and their disruption in psychiatric and neurodegenerative disorders. Annu Rev Neurosci 33:349–378. CrossRef Medline

Liu W, MacGrath SM, Koleske AJ, Boggon TJ (2012) Lysozyme contamination facilitates crystallization of a heterotrimeric cortactin-Arg-lysozyme complex. Acta Crystallogr Sect F Struct Biol Cryst Commun 68:154–158. CrossRef Medline

MacGrath SM, Koleske AJ (2012a) Arg/Abl2 modulates the affinity and stoichiometry of binding of cortactin to f-actin. Biochemistry 51:6644–6653. CrossRef Medline

MacGrath SM, Koleske AJ (2012b) Cortactin in cell migration and cancer at a glance. J Cell Sci 125:1621–1626. CrossRef Medline

Matus A (2000) Actin-based plasticity in dendritic spines. Science 290:754–758. CrossRef Medline

Meijering E (2010) Neuron tracing in perspective. Cytometry A 77:693–704. Medline

Meijering E, Jacob M, Sarria JC, Steiner P, Hirling H, Unser M (2004) Design and validation of a tool for neurite tracing and analysis in fluorescence microscopy images. Cytometry A 58:167–176. Medline

Miller AL, Wang Y, Mooseker MS, Koleske AJ (2004) The Abl-related gene (Arg) requires its F-actin-microtubule cross-linking activity to regulate lamellipodial dynamics during fibroblast adhesion. J Cell Biol 165:407–419. CrossRef Medline

Moresco EM, Koleske AJ (2003) Regulation of neuronal morphogenesis and synaptic function by Abl family kinases. Curr Opin Neurobiol 13:535–544. CrossRef Medline

Moresco EM, Scheetz AJ, Bornmann WG, Koleske AJ, Fitzsimonds RM (2003) Abl family nonreceptor tyrosine kinases modulate short-term synaptic plasticity. J Neurophysiol 89:1678–1687. Medline

Moresco EM, Donaldson S, Williamson A, Koleske AJ (2005) Integrin-mediated dendrite branch maintenance requires Abelson (Abl) family kinases. J Neurosci 25:6105–6118. CrossRef Medline

Mueller BK, Mack H, Teusch N (2005) Rho kinase, a promising drug target for neurological disorders. Nat Rev Drug Discov 4:387–398. CrossRef Medline

Nägerl UV, Eberhorn N, Cambridge SB, Bonhoeffer T (2004) Bidirectional

activity-dependent morphological plasticity in hippocampal neurons. Neuron 44:759–767. CrossRef Medline

Nakayama AY, Harms MB, Luo L (2000) Small GTPases Rac and Rho in the maintenance of dendritic spines and branches in hippocampal pyramidal neurons. J Neurosci 20:5329–5338. Medline

Newey SE, Velamoor V, Govek EE, Van Aelst L (2005) Rho GTPases, dendritic structure, and mental retardation. J Neurobiol 64:58–74. CrossRef Medline

Nodé-Langlois R, Muller D, Boda B (2006) Sequential implication of the mental retardation proteins ARHGEF6 and PAK3 in spine morphogenesis. J Cell Sci 119:4986–4993. CrossRef Medline

Parnass Z, Tashiro A, Yuste R (2000) Analysis of spine morphological plasticity in developing hippocampal pyramidal neurons. Hippocampus 10: 561–568. CrossRef Medline

Peacock JG, Couch BA, Koleske AJ (2010) The Abl and Arg non-receptor tyrosine kinases regulate different zones of stress fiber, focal adhesion, and contractile network localization in spreading fibroblasts. Cytoskeleton 67:666–675. CrossRef Medline

Redmond L (2008) Translating neuronal activity into dendrite elaboration: signaling to the nucleus. Neurosignals 16:194–208. CrossRef Medline

Rubinson DA, Dillon CP, Kwiatkowski AV, Sievers C, Yang L, Kopinja J, Rooney DL, Zhang M, Ihrig MM, McManus MT, Gertler FB, Scott ML, Van Parijs L (2003) A lentivirus-based system to functionally silence genes in primary mammalian cells, stem cells and transgenic mice by RNA interference. Nat Genet 33:401–406. CrossRef Medline

Ryu J, Liu L, Wong TP, Wu DC, Burette A, Weinberg R, Wang YT, Sheng M (2006) A critical role for myosin IIb in dendritic spine morphology and synaptic function. Neuron 49:175–182. CrossRef Medline

Saneyoshi T, Hayashi Y (2012) The Ca2+ and Rho GTPase signaling pathways underlying activity-dependent actin remodeling at dendritic spines. Cytoskeleton 69:545–554. CrossRef Medline

Saneyoshi T, Fortin DA, Soderling TR (2010) Regulation of spine and synapse formation by activity-dependent intracellular signaling pathways. Curr Opin Neurobiol 20:108–115. CrossRef Medline

Scarbrough PR, Files B, Carroll AJ, Quinlan RW, Finley SC, Finley WH (1988) Interstitial deletion of chromosome 1 [del(1)(q25q32)] in an infant with prune belly sequence. Prenat Diagn 8:169–174. CrossRef Medline

Schubert V, Da Silva JS, Dotti CG (2006) Localized recruitment and activation of RhoA underlies dendritic spine morphology in a glutamate receptor-dependent manner. J Cell Biol 172:453–467. CrossRef Medline

Sfakianos MK, Eisman A, Gourley SL, Bradley WD, Scheetz AJ, Settleman J, Taylor JR, Greer CA, Williamson A, Koleske AJ (2007) Inhibition of Rho via Arg and p190RhoGAP in the postnatal mouse hippocampus regulates dendritic spine maturation, synapse and dendrite stability, and behavior. J Neurosci 27:10982–10992. CrossRef Medline

Siton O, Ideses Y, Albeck S, Unger T, Bershadsky AD, Gov NS, Bernheim-Groswasser A (2011) Cortactin releases the brakes in actin- based motility by enhancing WASP-VCA detachment from Arp2/3 branches. Curr Biol 21:2092–2097. CrossRef Medline

Smart FM, Halpain S (2000) Regulation of dendritic spine stability. Hippocampus 10:542–554. CrossRef Medline

Sorra KE, Harris KM (2000) Overview on the structure, composition, function, development, and plasticity of hippocampal dendritic spines. Hippocampus 10:501–511. CrossRef Medline

Suo L, Lu H, Ying G, Capecchi MR, Wu Q (2012) Protocadherin clusters and cell adhesion kinase regulate dendrite complexity through Rho GTPase. J Mol Cell Biol 4:362–376.

Svitkina T, Lin WH, Webb DJ, Yasuda R, Wayman GA, Van Aelst L, Soderling SH (2010) Regulation of the postsynaptic cytoskeleton: roles in development, plasticity, and disorders. J Neurosci 30:14937–14942. CrossRef Medline

Tada T, Sheng M (2006) Molecular mechanisms of dendritic spine morphogenesis. Curr Opin Neurobiol 16:95–101. CrossRef Medline

Takano T, Yamanouchi Y, Mori Y, Kudo S, Nakayama T, Sugiura M, Hashira S, Abe T (1997) Interstitial deletion of chromosome 1q [del(1)(q24q25.3)] identified by fluorescence in situ hybridization and gene dosage analysis of apolipoprotein A-II, coagulation factor V, and antithrombin III. Am J Med Genet 68:207–210. CrossRef Medline

Tashiro A, Yuste R (2004) Regulation of dendritic spine motility and stability by Rac1 and Rho kinase: evidence for two forms of spine motility. Mol Cell Neurosci 26:429–440. CrossRef Medline

Tashiro A, Minden A, Yuste R (2000) Regulation of dendritic spine morphology by the rho family of small GTPases: antagonistic roles of Rac and Rho. Cereb Cortex 10:927–938. CrossRef Medline

Tolias KF, Duman JG, Um K (2011) Control of synapse development and plasticity by Rho GTPase regulatory proteins. Prog Neurobiol 94:133–148. CrossRef Medline

Van Aelst L, Cline HT (2004) Rho GTPases and activity-dependent dendrite development. Curr Opin Neurobiol 14:297–304. CrossRef Medline

Warren MS, Bradley WD, Gourley SL, Lin YC, Simpson MA, Reichardt LF, Greer CA, Taylor JR, Koleske AJ (2012) Integrin beta1 signals through Arg to regulate postnatal dendritic arborization, synapse density, and behavior. J Neurosci 32:2824–2834. CrossRef Medline

Xing L, Yao X, Williams KR, Bassell GJ (2012) Negative regulation of RhoA translation and signaling by hnRNP-Q1 affects cellular morphogenesis. Mol Biol Cell 23:1500–1509. CrossRef Medline

Yoshihara Y, De Roo M, Muller D (2009) Dendritic spine formation and stabilization. Curr Opin Neurobiol 19:146–153. CrossRef Medline

Zhang H, Macara IG (2008) The PAR-6 polarity protein regulates dendritic spine morphogenesis through p190 RhoGAP and the Rho GTPase. Dev Cell 14:216–226. CrossRef Medline

Zhang W, Benson DL (2000) Development and molecular organization of dendritic spines and their synapses. Hippocampus 10:512–526. CrossRef Medline